

## Generalized parton distributions of light nuclei

Sara Fucini · Matteo Rinaldi · Sergio Scopetta

Received: date / Accepted: date

**Abstract** The measurement of nuclear generalized parton distributions (GPDs) in hard exclusive processes, such as deeply virtual Compton Scattering (DVCS), will be one of the main achievements of a new generation of experiments at high luminosity, such as those under way at the Jefferson Laboratory (JLab) with the 12 GeV electron beam and, above all, those planned at the future Electron Ion Collider. The CLAS collaboration at JLab has recently demonstrated the possibility to disentangle the two different channels of nuclear DVCS, the coherent and incoherent ones, a first step towards the measurement of GPDs of nuclei and of bound nucleons, respectively, opening new exciting perspectives in the field. In this scenario, theoretical precise calculations, ultimately realistic, become mandatory. Light nuclei, for which realistic studies are affordable and conventional nuclear effects can be safely estimated, so that possible exotic effects can be exposed, play an important role. The status of the calculation of GPDs for light nuclei will be summarized, in particular for  $^3\text{He}$  and  $^4\text{He}$ , and some updates will be presented. The prospects for the next years, related to the new series of measurements at future facilities, will be addressed.

---

S. Fucini  
Department of Physics and Geology  
Perugia University and INFN, Perugia  
via A. Pascoli snc 06123 Perugia  
E-mail: sara.fucini@pg.infn.it

M. Rinaldi  
Department of Physics and Geology  
Perugia University and INFN, Perugia  
via A. Pascoli snc 06123 Perugia  
E-mail: matteo.rinaldi@pg.infn.it

S. Scopetta  
Department of Physics and Geology  
Perugia University and INFN, Perugia  
via A. Pascoli snc 06123 Perugia  
E-mail: sergio.scopetta@pg.infn.it

---

**Keywords** Few-Body Nuclei · Deep inelastic scattering · Exclusive processes

## 1 Introduction

The nucleus is a unique laboratory for fundamental studies of the QCD hadron structure [1]. For example, the extraction of the neutron information from light nuclei, essential for a precise flavor separation of parton distributions (PDFs), the measurement of nuclear PDFs, relevant for the analysis of nucleus-nucleus scattering aimed, e.g., at producing quark-gluon plasma, or the phenomenon of in-medium fragmentation, mandatory to unveil the dynamics of hadronization, require nuclear targets. Nevertheless, inclusive Deep Inelastic Scattering (DIS) experiments off nuclei have been unable to answer a few fundamental questions. Among those of interest in this paper, we list: (i) the quantitative microscopic explanation of the so called European Muon Collaboration (EMC) effect [2], i.e., the observed medium modification of the nucleon parton structure; (ii) the correct extraction of the structure of the neutron from nuclear data.

Novel coincidence measurements at high luminosity facilities, such as Jefferson Laboratory (JLab), have become recently possible, addressing a new era in the knowledge of the parton structure of nuclei [3]. An even more relevant improvement is expected with the operation of the future Electron-Ion Collider (EIC), based in the US [4]. In particular, two promising directions beyond inclusive measurements, aimed at unveiling the three dimensional (3D) structure of the bound nucleon, are deep exclusive processes off nuclei, and semi-inclusive deep inelastic scattering (SIDIS) involving nuclear targets. In deep exclusive processes, as those here addressed, one accesses the 3D structure in coordinate space, in terms of generalized parton distributions (GPDs). In the following, we will show how, in this way, a relevant contribution is expected to the solution of long standing problems, such as: (i) the non nucleonic contribution to nuclear structure, (ii) the quantitative explanation of the medium modification of the nucleon parton structure, or (iii) a precise flavor separation of the nucleon parton distributions.

The paper is structured as follows. The next section is dedicated to show in general which novel information one could obtain from the measurements of nuclear GPDs. In section 3, the role of few-body nuclear systems is illustrated. Known results are summarized and some updates are presented for  $^3\text{He}$  and  $^4\text{He}$  nuclei. The perspectives in this field of research are eventually described.

## 2 Learning from nuclear GPDs

Excellent introduction to GPDs, quantities initially defined in refs. [5, 6, 7] and measured in hard exclusive processes, can be found in refs. [8, 9, 10, 11]. Among their most relevant properties, we remind just the ones of interest in the present paper. To fix the ideas, let us think to deeply virtual Compton

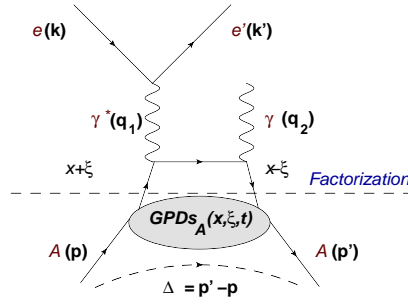


**Fig. 1** The handbag contribution to the coherent DVCS process off a nucleus  $A$ .

scattering (DVCS), depicted in Fig. 1 in the handbag approximation. If the initial photon virtuality,  $Q^2 = -q_1^2 = -(k - k')^2$ , is much larger than  $-t = -\Delta^2 = -(p - p')^2$ , the momentum transferred to the hadronic system with initial (final) 4-momentum  $p(p')$ , the hard vertex of the “handbag” diagram shown in Fig. 1 can be studied perturbatively. The soft part is parametrized in terms of the GPDs of the target, which depend on  $t = \Delta^2$ , on the so-called skewness  $\xi = -\Delta^+/P^+$ , i.e., the difference in plus momentum fraction between the initial and the final states, and on  $x$ , the average plus momentum fraction of the struck parton with respect to the total momentum, not experimentally accessible (the notation  $a^\pm = (a_0 \pm a_3)/\sqrt{2}$  is used). The average photon four momentum is  $q = (q_1 + q_2)/2$ , while the total target momentum is  $P = p + p'$ . The number of leading-twist GPDs for a target  $A$  with spin  $J_A$  is  $2(2J_a + 1)^2$ , one half of which are chiral odd. In this paper we will deal only with chiral even ones, i.e., for example, for a spin 1/2 target, the two spin-independent ones, defined in terms of an off forward quark light-cone correlator:

$$\frac{1}{2} \int \frac{d\xi^-}{2\pi} e^{ixP^+\xi^-} \langle P' s' | \bar{\psi}_q(0, \xi^-/2, 0_\perp) \gamma^+ \psi_q(0, \xi^-/2, 0_\perp) | P s \rangle = H_q(x, \xi, \Delta^2) \frac{1}{2} \bar{u}(P', s') \gamma^+ u(P, s) + E_q(x, \xi, \Delta^2) \frac{1}{2} \bar{u}(P', s') \frac{i\sigma^{+\nu} \Delta_\nu}{2M} u(P, s), \quad (1)$$

and the spin dependent ones,  $\tilde{H}_q$  and  $\tilde{E}_q$ , obtained from the above expression substituting  $\gamma^+$  and  $\sigma^{+\nu} \Delta_\nu$  by  $\gamma^+ \gamma_5$  and  $\gamma_5 \Delta^+$ , respectively.

The  $x$ -integral of the GPDs yields proper form factors (ffs). For example,  $H_q$  and  $E_q$  are related to the Dirac and Pauli ones, respectively. More in general, Lorentz invariance determines the polynomiality property, stating that the  $n$ -moments of GPDs are polynomials in  $\xi$  of order  $n + 1$ .

The forward limit,  $\Delta^2 \rightarrow 0$ , of the GPDs  $H_q$  and  $\tilde{H}_q$ , provides the helicity-independent and helicity-dependent PDFs, respectively.

Initially introduced as a tool towards the understanding of the spin content of the proton, being  $H_q$  and  $E_q$  related to the total angular momentum through the Ji's sum rule [6], another crucial property of GPDs is the possibility to allow the so-called tomography of the target. As demonstrated in

ref. [12], the GPD  $H_q$  at zero skewness, Fourier transformed to the impact parameter space, represents the number density of the partons with a given longitudinal momentum fraction at a given transverse distance from the center of the target. Obviously, having at hand tomography data for the proton, for the nucleus and for the bound proton, possible differences in the distributions of the partons in the transverse plane between these three systems would provide a pictorial representation of the realization of the EMC effect. In principle, the tomography of the nucleus and that of the bound proton are accessible through the so called coherent DVCS, where the nucleus is detected intact in the final state, and incoherent DVCS, with the detection of a bound proton in the final state. Nuclear DVCS is therefore very promising in this direction.

The study of DVCS has therefore many virtues but it is very difficult. Hard exclusive processes have obviously very small cross sections and in the final state one has at the same time slow and fast systems to be detected, which makes analyses very involved. On the top of that, the average momentum fraction  $x$  is not accessible and the DVCS amplitude is integrated on this variable, being proportional to the so-called Compton form factors (CFFs), discussed in the following sections. One should notice that in the inclusive case, i.e., in DIS, the differential cross section is proportional to the PDFs, which makes their measurements much easier than that of GPDs, which have to be deconvoluted from the CFFs.

Despite of these drawbacks, a first glance at the free proton tomography, obtained with little model dependence, has been obtained [13]. The nuclear one, after the important achievement of the CLAS collaboration at JLab, with the first separation of coherent and incoherent channels in DVCS off  $^4\text{He}$  [14, 15], should be accessed in the next years.

The relevance of the coherent channel has been stressed in [3]. Here the main advantages are just listed. Besides the already mentioned nuclear tomography, along the lines of [12], one could 1) compare data with precise impulse approximation (IA) calculations, possible for few body nuclei, to expose non nucleonic d.o.f., according to an idea initially presented in [16]; 2) access information on the nuclear energy momentum tensor (EMT) and the  $d$ -term (initial idea in [17], more recent developments in [18], and a report in [19]); we observe that a positron beam, whose use at JLab and at the EIC is under discussion [20], would help to access this information; 3) access gluon gpdfs in nuclei, haunting possible gluon d.o.f. [21]; 4) extract pieces of information for the free neutron, possible using specific nuclei and specific polarization setups in the experiments [22]; 5) study a predicted peculiar shadowing at low  $x$  [23].

Two of these relevant possibilities, beyond tomography, are presented in the two following subsections.

## 2.1 Non-nucleonic degrees of freedom in nuclei from nuclear GPDs

The knowledge of GPDs would permit the investigation of the interplay of nucleon and parton degrees of freedom in the nuclear wave function [16]. In standard DIS off a nucleus with four-momentum  $P_A$  and  $A$  nucleons of mass  $M$ , this information can be accessed in the region where  $x_{Bj} = \frac{Q^2}{2M\nu}$  is greater than 1,  $\nu$  being the energy transfer in the laboratory system. In this region, kinematically forbidden for a free proton, extremely fast quarks are tested and measurements are therefore very difficult, because of vanishing cross-sections. As explained in [16, 24], a similar information can be accessed in DVCS at lower values of  $x_{Bj}$ .

To understand this aspect, it is instructive to analyze coherent DVCS in IA. Let us think to unpolarized DVCS off a nucleus with  $A$  nucleons, which is dominated by the GPD  $H_q^A$ . This case has been treated in [24] for the deuteron target, in [25] for spin-0 nuclei, in [26] for nuclei with spin up to 1, in [27] for  ${}^3\text{He}$  and in [28, 29] for  ${}^4\text{He}$ . In IA,  $H_q^A$  is obtained as a convolution between the non-diagonal spectral function of the internal nucleons and the GPD  $H_q^N$  of the nucleons themselves. The process is depicted in Fig. 1 for coherent DVCS, assuming the handbag approximation. Here, one parton belonging to a given nucleon interacts with the probe and it is then reabsorbed, with an additional momentum  $\Delta$ , by the same nucleon, without further re-scattering with the recoiling system. Finally, the interacting nucleon is reabsorbed back into the nucleus. The main assumptions of IA are: (i) the nuclear operator is just the sum of single nucleon free operators, i.e., there are only explicit nucleonic d.o.f.; (ii) the interaction of the debris originating by the struck nucleon with the remnant ( $A - 1$ ) system is disregarded (we are close to the Bjorken limit); (iii) the coupling of the virtual photon with the spectator ( $A-1$ ) system is neglected (given the high momentum transfer), (iv) the effect of the boosts is not considered (they can be properly taken into account in a light-front framework). Within all these conditions, the GPD  $H_q^A$  can be written in the form:

$$H_q^A(x, \xi, \Delta^2) = \sum_N \int_x^1 \frac{dz}{z} h_N^A(z, \xi, \Delta^2) H_q^N\left(\frac{x}{z}, \frac{\xi}{z}, \Delta^2\right) \quad (2)$$

where

$$h_N^A(z, \xi, \Delta^2) = \int dE \int d\mathbf{p} P_N^A(\mathbf{p}, \mathbf{p} + \mathbf{\Delta}, E) \delta\left(z + \xi - \frac{p^+}{P^+}\right) \quad (3)$$

is the off-diagonal light-cone momentum distribution of the nucleon  $N$  in the nucleus  $A$ .  $P_N^A(\mathbf{p}, \mathbf{p} + \mathbf{\Delta}, E)$  is the one-body off-diagonal spectral function. The latter quantity has been introduced and calculated for the  ${}^3\text{He}$  target first in [27]. Here,  $E = E_{min} + E_R^*$  is the so called removal energy, with  $E_{min} = |E_A| - |E_{A-1}|$  and  $E_R^*$  is the excitation energy of the nuclear recoiling system.

One should notice that eq. (2) fulfills the general properties of GPDs, i.e., the forward limit reproduces the standard nuclear PDF in IA and the

the first  $x$ -moment yields the IA form factor. The polynomiality property is formally fulfilled, however, since in these calculations use has been made of non-relativistic wave functions, this feature is actually valid only at order  $O(\frac{p^2}{m^2})$ . In particular, by taking the forward limit ( $\Delta^2 \rightarrow 0, \xi \rightarrow 0$ ) of eq. (2), one gets the expression which is usually found, for the parton distribution  $q_A(x)$ , in the IA analysis of unpolarized DIS:

$$q_A(x_{Bj}) = H_q^A(x_{Bj}, 0, 0) = \sum_N \int_{x_{Bj}/A}^1 \frac{d\tilde{z}}{\tilde{z}} f_N^A(\tilde{z}) q_N\left(\frac{x_{Bj}}{\tilde{z}}\right). \quad (4)$$

In the latter equation,

$$f_N^A(\tilde{z}) = h_N^A(\tilde{z}, 0, 0) = \int dE \int d\mathbf{p} P_N^A(\mathbf{p}, E) \delta\left(\tilde{z} - \frac{p^+}{P^+}\right) \quad (5)$$

is the light-cone momentum distribution of the nucleon  $N$  in the nucleus,  $q_N(x) = H_q^N(x, 0, 0)$  is the distribution of the quarks of flavor  $q$  in the nucleon  $N$  and  $P_N^A(\mathbf{p}, E)$  is the one body diagonal spectral function.

In a typical IA calculation, the light-cone momentum distribution  $f_N^A(z)$  turns out to be strongly peaked around the value  $z \simeq 1/A$ . Therefore, in order to investigate the effects of nucleons with large “plus” momentum fraction, one needs to consider regions where therefore to be at  $z > 1/A$ . Looking at the lower integration limit in eq. (4), it is clear that, in the DIS case, this occurs at  $x_{Bj} > 1$ , where the cross sections are very small. Recent analyses of inclusive data at  $x_{Bj} > 1$  have only been able to quantify the number of such fast correlated nucleons, but without addressing their internal structure [30, 31, 32].

In the coherent channel of a hard exclusive process, when the recoiling nucleus does not breakup, a longitudinal momentum is transferred, tuned by the kinematical variable  $\xi$ , which can be larger than the narrow width of the light cone momentum distribution, so that the predicted DVCS cross section is vanishing. In [24], for the deuteron case, it is estimated that the IA predicts a vanishing cross section already for  $x_{Bj} \simeq 0.2$ , i.e. for  $\xi \simeq 0.1$ . By experimentally tuning  $\xi$  in a coherent DVCS process one could therefore explore at relatively low values of  $x_{Bj}$  contributions to the GPDs not included in IA, i.e., accessing non nucleonic degrees of freedom generating correlations at parton level or other exotic effects. These studies could contribute to explain the nuclear EMC effect.

## 2.2 Spatial distribution of energy, momentum and forces experienced by partons in nuclei

In this section, we shall discuss how the lowest Mellin moments of GPDs provide us with information about the spatial distribution of energy, momentum and forces experienced by quarks and gluons inside nuclei. This idea, leading to predictions to be experimentally tested, has been developed initially in [17].

To be specific, let us consider a spin-1/2 hadronic target, e.g. a nucleon. All spin independent equations apply to the spin-0 targets as well.

The  $x$ -moments of the GPDs are related to three scalar ffs [6], in terms of which the matrix elements of the EMT can be parametrized. The ff we are interested in, usually called  $d^Q(t)$ , is related to the first Mellin moment of the unpolarized GPD [6]:

$$\int_{-1}^1 dx x H(x, \xi, t) = M_2^Q(t) + \frac{4}{5} d^Q(t) \xi^2. \quad (6)$$

Thanks to this relation,  $d^Q(t)$  can be studied in hard exclusive processes. In particular,  $d^Q(t)$  contributes with an  $x_{Bj}$  independent term to the real part of the DVCS amplitude, which is accessible through the beam charge asymmetry [33], measurable using electron and positron beams. At the same time, this ff is related to the so-called D-term in the parametrization of the GPDs [34]. Let us remind that at small  $x_{Bj}$ ,  $t$  and to the leading order in  $\alpha_s(Q)$ , the  $x_{Bj}$  dependent contribution to the real part of the DVCS amplitude is basically given by the ‘‘slice’’  $H_q(\xi, \xi, t)$  of quark GPD, measurable through the DVCS beam spin asymmetry (BSA)

$$A_{LU} = \frac{d\sigma^+ - d\sigma^-}{d\sigma^+ + d\sigma^-}, \quad (7)$$

where the differential cross sections  $d\sigma^\pm$  for the beam helicities ( $\pm$ ) appear.

In principle, the ff  $d^Q(t)$  can be therefore extracted from combined data of DVCS beam spin asymmetry and beam charge asymmetry, whose measurements requires positron beams (see, e.g., ref. [20] for the perspectives in the future use of positrons). It can be shown that  $d^Q(t)$  is related to the traceless part of  $T_{ik}^Q(\mathbf{r}, \mathbf{s})$ , which characterizes the spatial distribution (averaged over time) of shear forces experienced by quarks in the nucleon [34]. In ref. [34], to illustrate the physics of  $d^Q(t)$ , a simple model of a large nucleus has been considered. In this framework, as an example, use has been made of a liquid drop model for a nucleus, with sharp edges. In this case one gets  $d(0) \sim A^{7/3}$ , i.e. it rapidly grows with the atomic number. This fact implies that the contribution of the D-term to the real part of the DVCS amplitude grows with the atomic number as  $A^{4/3}$ . This should be compared to the behavior of the amplitude  $\sim A$  in IA and experimentally checked by measuring the charge beam asymmetry in coherent DVCS on nuclear targets. A similar  $A$  dependence of  $d(0)$  has been predicted also in a microscopic evaluation of nuclear GPDs for spin-0 nuclei in the framework of the Walecka model [35]. The meson (non-nucleonic) degrees of freedom were found to strongly influence DVCS nuclear observables, in the HERMES kinematics.

The first experimental study of DVCS on nuclei of noble gases, reported in [36], was not able to observe the predicted  $A$  dependence. The data are anyway affected by sizable error bars and more precise DVCS experiments could provide information on nuclear modifications of the EMT ffs.

### 3 GPDs of few body nuclei

Since conventional nuclear effects, if not properly evaluated, can be easily mistaken for exotic ones, light nuclei, for which realistic calculations are possible and conventional nuclear effects can be exactly calculated, play a special role. Besides, light nuclei impose their relevance in the extraction of the neutron information, necessary to perform a clean flavor separation of GPDs, crucial to test QCD fundamental symmetries and predictions. We note that an indirect procedure to constrain the neutron GPDs using coherent and incoherent DVCS off nuclei has been proposed in ref. [37].

#### 3.1 The deuteron

The deuteron, being a spin 1 nucleus, has a very rich spin structure and in particular, as detailed in the introduction, 18 leading twist GPDs. It offers therefore unique possibilities. However, since the deuteron is very weakly bound, it is not expected to be suitable to investigate nuclear medium modifications. It is the first natural candidate to access the neutron information, using mainly incoherent DVCS. In that channel, FSI could hinder their extraction, and specific kinematical regions, where FSI is known to be less relevant, have to be therefore selected. To this aim, dedicated theoretical estimates of FSI in this channel are very important. An experiment of this kind has been performed at JLab after the 12 GeV upgrade and the analysis is in progress [38]. Another promising possibility, for the measurement of DVCS off the neutron, to be detailed in forth-coming proposals [39], is that offered by the detection of a slow recoiling proton in DVCS off the deuteron. In this case, the experimental setup, successfully used in spectator SIDIS by the BONUS collaboration at JLab [40], will be exploited. Among the nuclear systems, the deuteron obviously represents the easiest to treat theoretically. A realistic nuclear description and a light-front (LF) relativistic implementation of IA are available. We recall that the twist-2 deuteron GPDs have been first introduced in in ref. [16]. Then, in ref. [24], the latter quantities have been evaluated in IA on the light cone together with the related coherent DVCS cross section. In addition, a specific spin sum rule has been discussed in ref. [41]. The deuteron will not be further discussed in this paper. The reader interested in recent developments can consult the discussion of transversity GPDs in ref. [42]; the fulfillment of polynomiality in calculations of deuteron GPDs in ref. [43]; the EMT for the deuteron in ref. [44].

#### 3.2 $^3\text{He}$

Trinucleons, having spin and isospin  $1/2$  as the nucleon, are suitable to access isospin and flavor dependence of nuclear effects [27, 45]. Here we discuss the advantages offered by trinucleons targets and beams. For these light nuclei realistic IA calculations are available and the off-diagonal spin-dependent

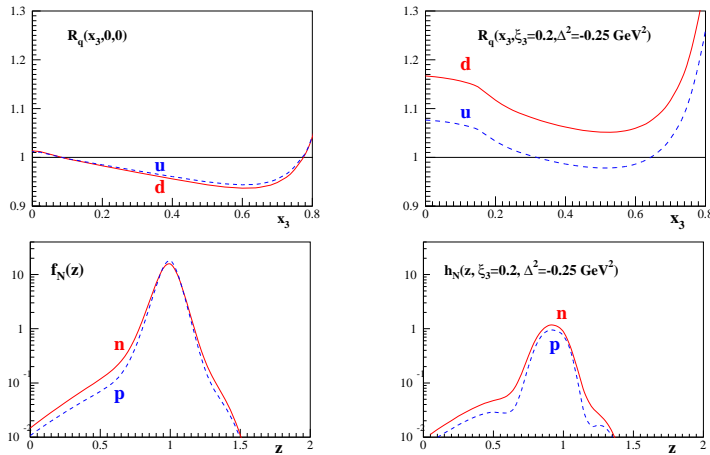


**Fig. 2** Upper left panel: the dashed (full) line represents the ratio of the  ${}^3\text{He}$  GPD  $H$  to the corresponding quantity of the constituent nucleons (2 protons and one neutron), for the  $u$  ( $d$ ) flavor, in the forward limit, as a function of  $x_3 = 3x$ . Lower left panel: the dashed (full) line represents the light cone momentum distribution, eq. (5), for the proton (neutron) in  ${}^3\text{He}$ . Upper right panel: the same as in the upper left panel, but at off-forward kinematics:  $t = -0.25 \text{ GeV}^2$  and  $\xi_3 = 3\xi = 0.2$ . Lower right panel: the dashed (full) line represents the light cone off diagonal momentum distribution, eq. (3), for the proton (neutron) in  ${}^3\text{He}$  at the same off-forward kinematics.

spectral function has been calculated [27, 45, 22, 46, 47]. Moreover, a relativistic treatment of the above quantity has been developed, for the moment only in the forward case, in ref. [48]. Let us remark that relativistic effects could be relevant in the calculations of PDFs and related quantities. In addition, the specific spin structure of  ${}^3\text{He}$  allows to extract the neutron spin-dependent GPDs, by properly taking into account conventional nuclear effects.

As shown in section 1, the conventional treatment of nuclear GPDs, through the IA, involves a non-diagonal nuclear spectral function. Despite its complicated dependence on the momentum and removal energy, the latter can be exactly evaluated for  ${}^3\text{He}$ . Therefore, such a nucleus is very suitable to realistically study polarization effects and to attempt a precise flavor separation of GPDs, being not an isoscalar target.

A realistic microscopic calculation of the unpolarized quark GPD of the  ${}^3\text{He}$  nucleus has been presented in ref. [27]. The proposed scheme points to the coherent channel of hard exclusive processes. Nuclear effects, evaluated within the AV18 potential [49], are found to be larger than in the forward case and get bigger and bigger with increasing  $t$  ( $\xi$ ) and keeping  $\xi$  ( $t$ ) fixed. Besides, the obtained GPD cannot be factorized into  $t$ -dependent and  $t$ -independent terms, as suggested by prescriptions proposed for finite nuclei [26].

In ref. [45] the analysis has been extended, showing that other conventional nuclear effects, such as isospin and binding ones, or the uncertainty related to the use of a given nucleon-nucleon potential, are rather bigger than in the

forward case. An example is shown in Fig. 2. As one can see, these effects increase when the light-cone momentum distributions, eqs. (3) and (5), depart from a delta-like behaviour, as it happens in the non-forward case. In addition, nuclear effects, for the  $u$  ( $d$ ) flavor, follow the path of the proton (neutron) light-cone momentum distributions. Future experimental observations of this behaviour, a typical prediction of a realistic conventional IA approach, would provide relevant information on the reaction mechanism of DIS off nuclear targets. Let us point out that these kind of effects could not be observed in isoscalar targets, such as  $^2\text{H}$  or  $^4\text{He}$ .

In ref. [46] the  $E$  GPD of  $^3\text{He}$  has been calculated following the line of ref. [27]. Let us remark that the GPDs  $H$  and  $E$  are involved in the Ji's sum rule which allows to extract information on the parton angular momentum of the system. One of the main outcomes of the analysis is that the neutron contribution is the dominant one to the GPD  $E$  and in particular to the combination  $H + E$ . We recall that the  $^3\text{He}$  magnetic form factor can be obtained as the first moment of  $H + E$  and, moreover, such a combination enters the Ji's sum rule. Therefore, these results confirmed, also in the case of DVCS, that  $^3\text{He}$  is an ideal target to access properties related to the polarization of the neutron. In fact, a polarized  $^3\text{He}$  nucleus is, to an extent of 90%, equivalent to a polarized neutron. Furthermore, in ref. [22], a technique, able to take into account the nuclear effects included in an IA analysis, and to safely extract the neutron information, has been proposed. In particular it has been shown that such a procedure works in the relevant kinematic conditions of possible measurements. A similar technique has been successfully tested also for the extraction of the  $\tilde{H}$  GPD of the neutron from the corresponding quantity of  $^3\text{He}$  [47]. This investigation would require coherent DVCS off polarized  $^3\text{He}$ , a challenging but not impossible measurement at present facilities. Thanks to these observations, coherent DVCS should be considered as a golden process to access the neutron GPDs and, in turn, the total angular momentum of the quarks in the neutron. Indeed, the  $E$  GPD of isoscalar targets, such as  $^2\text{H}$  and  $^4\text{He}$ , is very small and, therefore, they are not suitable for this purpose. However, the measurement of this GPD would require a transverse polarization of  $^3\text{He}$ , a very difficult setup for the coherent channel at the present facilities. Nevertheless, in order to guide future experimental analyses, at JLab and at the future EIC, we are at present using the calculated GPDs to estimate the actual observables to be measured in experiments. As a preliminary outcome of these studies, we show in Fig. 3 the beam-spin asymmetry for the coherent DVCS processes off  $^3\text{He}$ , calculated in the kinematical configurations listed in Tab. 1, similar to those already studied at JLab using  $^4\text{He}$  and discussed in the next section. Let us point out that together with the AV18 spectral function previously discussed, use has been made of the nucleon GPDs of ref. [50] to evaluate the nuclear GPDs. Predictions for the relative cross-section will be available soon, also in the EIC kinematics.

In closing let us stress that  $^3\text{He}$  represents a unique system for nuclear GPD studies: its conventional structure is completely under control, so that the interplay of conventional and exotic effects can be exposed to provide hints

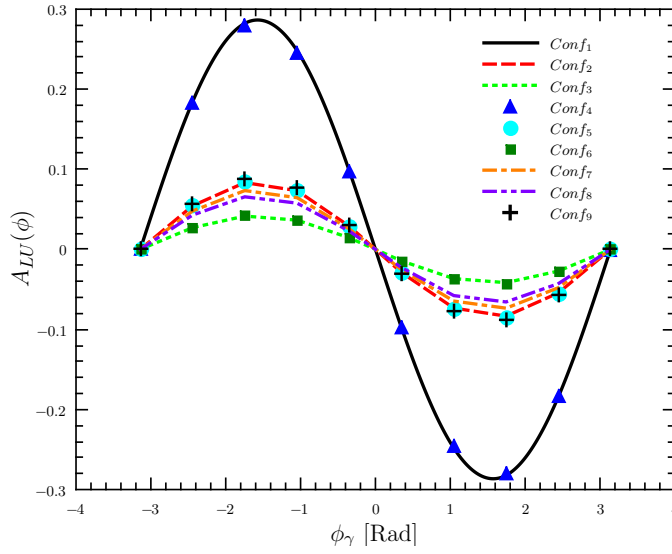


**Fig. 3** The preliminary  $^3\text{He}$  beam-spin asymmetry evaluated for the 9 kinematical configurations given in Tab. 1. Here  $\phi_\gamma = \phi - \pi$ , with  $\phi$  the azimuthal angle between the hadron and lepton planes.

$x_B$	$Q^2$ [GeV $^2$ ]	$t$ [GeV $^2$ ]	$\xi$	Configuration
0.132	1.18	-0.095	0.070664	1
0.171	1.45	-0.099	0.093494	2
0.225	1.84	-0.106	0.126761	3
0.134	1.15	-0.096	0.071811	4
0.171	1.42	-0.099	0.093494	5
0.223	1.87	-0.106	0.125492	6
0.159	1.37	-0.081	0.086366	7
0.179	1.51	-0.094	0.098298	8
0.193	1.61	-0.126	0.106807	9

**Table 1** The kinematical configurations adopted to evaluate the beam-spin asymmetry.

on them, when heavier nuclear targets are used. Besides, polarized  $^3\text{He}$  is a convenient effective polarized neutron whose GPDs  $E$  and  $\tilde{H}$  could be easily extracted from the corresponding  $^3\text{He}$  quantities, at low  $t$ , in a rather model independent way. To this aim, the measurements of polarized coherent DVCS would be required, certainly challenging but, in particular for the extraction of  $\tilde{H}$ , unique and not prohibitive. This is true especially at the future EIC, where polarized light ion beams are planned to circulate.

### 3.3 $^4\text{He}$

In  $^4\text{He}$ , the binding energy per nucleon is significantly larger than that of the other light nuclei so that such nucleus exhibits the features of a typical nuclear system. For this reason,  $^4\text{He}$  can be considered as a prototype system to study the partonic structure of typical nuclear targets. Besides, the study of such nucleus exhibits many advantages: from one side, being spinless, it has a straightforward theoretical description in terms of one leading-twist GPD in the chiral even sector and realistic (non relativistic) descriptions, although challenging, can be developed. From the other side, the experimental analyses are easier with respect to other targets like the  $^3\text{He}$  nucleus, as discussed in the previous section. In facts, the two DVCS channels, the coherent and the incoherent ones, have been recently disentangled at JLab by the CLAS collaboration [14, 15]. Several theoretical models have been developed to explain such reaction mechanisms [25, 51]. The most recent calculations within, an Av18 [49] + UIX [52] semi-realistic nuclear description, has been presented in ref. [29] for the coherent channel, and in refs. [53, 54] for the incoherent one. These models turn out to be able to successfully reproduce experimental data for  $A_{LU}$  in the kinematical range unraveled at JLab, i.e. the valence region. A deeply investigation of the region at small  $x_{Bj}$  is going on as these effects could be sizeable and useful for the explanation of the EMC effect in the shadowing region, that could be probed by the forth-coming EIC. Besides, for their features, these models have been used to develop a new Monte Carlo event generator for the DVCS process off  $^4\text{He}$  in view of the big experimental program that will be carried out at the EIC. In the Wiki page [55], the main results from the generation of the events for the coherent channel are shown.

Let us present our main results for these processes. As stated before in this paper, the  $x$  dependence of GPDs cannot be experimentally accessed. Nevertheless, the so called Compton Form Factor (CFF)  $\mathcal{H}$  can be extracted from measured observables. As a matter of facts, GPDs ( $H_q$ ) are hidden in the imaginary and the real part of such objects defined ( $e_q$  being the quark electric charge) as:

$$\Im\mathcal{H}(\xi, t) = \sum_q e_q^2 [H_q^{4He}(\xi, \xi, \Delta^2) - H_q^{4He}(-\xi, \xi, \Delta^2)], \quad (8)$$

$$\Re\mathcal{H}(\xi, t) = \text{Pr} \sum_q e_q^2 \int_{-1}^1 dx \left( \frac{1}{\xi - x} - \frac{1}{\xi + x} \right) H_q^{4He}(x, \xi, t), \quad (9)$$

respectively. The experimental observable which gives access to the above quantities is the beam spin asymmetry (BSA), defined in eq. (7).

In the following, we will summarize the main results obtained from a realistic calculations of conventional effects for the BSA within a plane wave impulse approximation approach.

### 3.3.1 Coherent DVCS channel

The most general coherent DVCS process  $A(e, e'\gamma)A$  allows to study the partonic structure of the recoiling whole nucleus  $A$  through the formalism of GPDs. In the IA scenario presented above, a workable expression for the quantity  $H_q^{4He}(x, \xi, \Delta^2)$ , the GPD of the quark of flavor  $q$  in the  ${}^4\text{He}$  nucleus, is obtained as a convolution between the GPDs  $H_q^N$  of the quark of flavor  $q$  in the bound nucleon  $N$  and the off-diagonal light-cone momentum distribution of  $N$  in  ${}^4\text{He}$  and reads

$$H_q^{4He}(x, \xi, \Delta^2) = \sum_N \int_{|x|}^1 \frac{dz}{z} h_N^{4He}(z, \xi, \Delta^2) \mathbf{H}_q^N \left( \frac{x}{z}, \frac{\xi}{z}, \Delta^2 \right). \quad (10)$$

In the previous equation,  $\mathbf{H}_q^N = \sqrt{1 - \xi^2} [H_q^N - \frac{\xi^2}{1 - \xi^2} E_q^N]$  has been evaluated using the GPD model given in refs. [50, 56]. Given in the kinematical range accessible at JLab, the contribution of the GPD  $E_q^N$  is supposed to be negligible and in ref. [29], only the contribution of the GPD  $H_q^N$  has been taken into account. Here, for the first time, both the  $H_q^N$  and the  $E_q^N$  GPD contributions have been accounted, as it can be seen in Figs. 4- 5. Then, the light cone momentum distribution in Eq (10) is defined as

$$h_N^{4He}(z, \Delta^2, \xi) = \int dE \int d\mathbf{p} P_N^{4He}(\mathbf{p}, \mathbf{p} + \mathbf{\Delta}, E) \delta \left( z - \frac{\bar{p}^+}{P^+} \right), \quad (11)$$

where the off diagonal spectral function  $P_N^{4He}(\mathbf{p}, \mathbf{p} + \mathbf{\Delta}, E)$  represents the probability amplitude to have a nucleon with momentum  $\mathbf{p}$  that leaves the nucleus, generating an excited recoiling system with energy  $E_R^* = E - |E_A| + |E_{A-1}|$ , with  $|E_A|$  and  $|E_{A-1}|$  the nuclear binding energies, and then goes back with a momentum transfer  $\mathbf{\Delta}$ . In order to have a full realistic evaluation of  $P_N^{4He}$ , an exact description of all the  ${}^4\text{He}$  spectrum, including three-body scattering states, is needed. Though, it represents a demanding few body problem whose complete evaluation is still going on. Old results in the diagonal case can be found in refs. [57, 58]. For this reason, as an intermediate step, in the present calculation a model of the nuclear non-diagonal spectral function [59], based on the momentum distribution corresponding to the Av18 NN interaction ref. [49] and including 3-body forces [52], has been used for the excited 3- and 4- body states. For the ground state, exact wave functions of 3- and 4-body systems [60, 61], evaluated along the scheme of ref. [62], have been considered. Before showing the comparison with data, we remark that checks for the nuclear charge form factor and for nuclear parton distributions have been successfully performed. Then, the comparison of our model for  $H_q^{4He}$  with the measured observables has been achieved evaluating numerically eqs. (8,9). The obtained results are depicted in Figs. 4. Finally, also the BSA of the coherent DVCS,

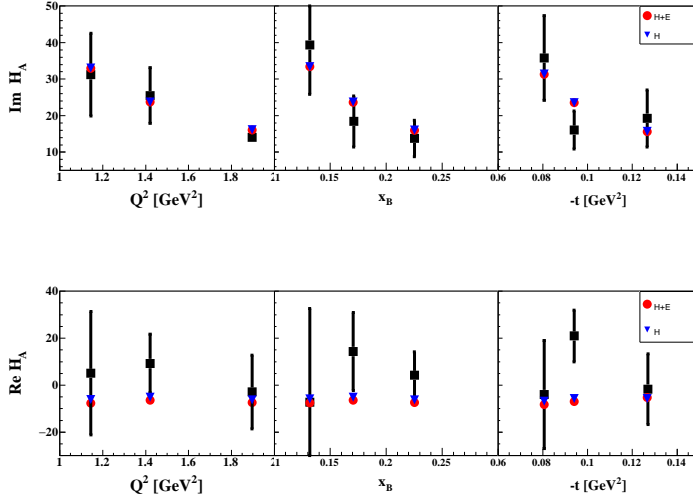


**Fig. 4** Imaginary (upper panel) and real part (lower panel) of the CFF for  $^4\text{He}$ : results of ref. [29] (blue triangles) and new results including also the GPD E (red dots) compared with data (black squares) [14]. The quantity is shown in the experimental  $Q^2$ ,  $x_B = Q^2/(2M\nu)$  and  $t = \Delta^2$  bins, respectively.

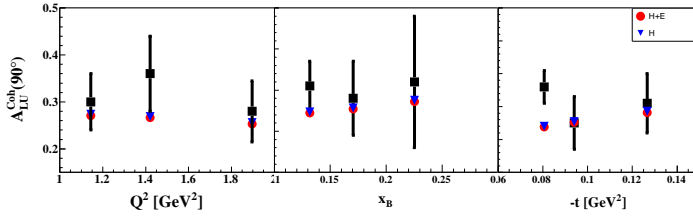


**Fig. 5**  $^4\text{He}$  azimuthal beam-spin asymmetry  $A_{LU}(\phi = 90^\circ)$ : results of ref. [29] (blue triangles) and new results including also the GPD  $E_N^q$  (red dots), compared with data (black squares) [14]. From left to right, the quantity is shown in the experimental  $Q^2$ ,  $x_B = Q^2/(2M\nu)$  and  $t = \Delta^2$  bins, respectively

i.e.

$$A_{LU}(\phi) = \frac{\alpha_0(\phi) \Im m(\mathcal{H}_A)}{\alpha_1(\phi) + \alpha_2(\phi) \Re e(\mathcal{H}_A) + \alpha_3(\phi) \left( \Re e(\mathcal{H}_A)^2 + \Im m(\mathcal{H}_A)^2 \right)}, \quad (12)$$

where  $\alpha_i(\phi)$  are kinematical coefficients defined in ref. [26], has been calculated and compared with the experimental data. As shown in Fig. 5, a very

good agreement is found with the data. These results lead us to conclude that a careful analysis of the reaction mechanism in terms of basic conventional ingredients is successful at the present experimental accuracy without requiring the use of exotic arguments, such as dynamical off-shellness.

### 3.3.2 Incoherent DVCS channel

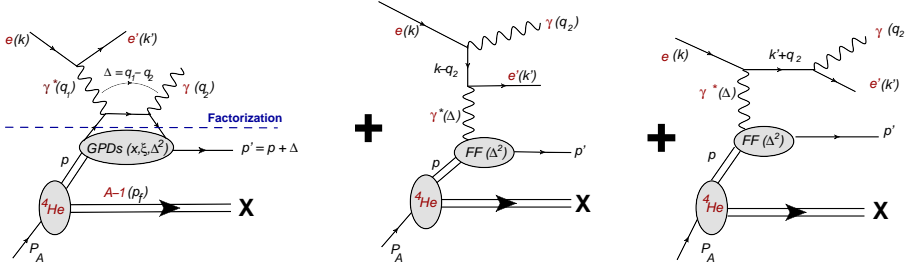


**Fig. 6** Incoherent DVCS off  ${}^4\text{He}$  in IA. To the left, pure DVCS contribution; to the right the two Bethe Heitler terms.

In the process  $A(e, e' \gamma p)X$  depicted in Fig. 6, the parton structure of the kicked out bound proton can be studied. For a complete evaluation of eq. (7), the expression of the cross-section for a DVCS process off a bound proton in  ${}^4\text{He}$  is required. In the IA scenario, only the kinematical off-shellness of the initial bound proton has been accounted for. In this way, a convolution formula for the differential cross has been derived, and it reads

$$d\sigma^\pm \equiv \frac{d\sigma_{Inc}^\pm}{dx_{Bj} dQ^2 d\Delta^2 d\phi} = \int_{exp} dE d\mathbf{p} P^{4He}(\mathbf{p}, E) |\mathcal{A}^\pm(\mathbf{p}, E, K)|^2 g(\mathbf{p}, E, K). \quad (13)$$

In the equation above,  $K$  is the set of kinematical variables  $\{x_{Bj}, Q^2, t, \phi\}$  probed in the experiment that selects only the relevant part of the diagonal spectral function  $P_N^{4He}(\mathbf{p}, E)$ , which has therefore to be integrated only in the selected experimental range  $exp$ . Moreover, the quantity  $g(\mathbf{p}, E, K)$  is a complicated function, whose derivation is detailed in ref. [54]. Finally, in the above equation, the squared amplitude includes three different terms, i.e.  $\mathcal{A}^2 = T_{DVCS}^2 + T_{BH}^2 + \mathcal{I}_{DVCS-BH}$  as shown in Fig. 6 and each contribution has to be evaluated for an initially moving proton. The amplitude addressed in refs. [53, 54] generalize those obtained for a proton at rest (see ref. [10]). Details on the main assumptions here adopted are summarized in refs. [53, 54]. Since in the kinematical range probed at JLab, the DVCS contribution is smaller than the BH term, information on the partonic structure of the target can be inferred only through the interference DVCS-BH term. In this way, the

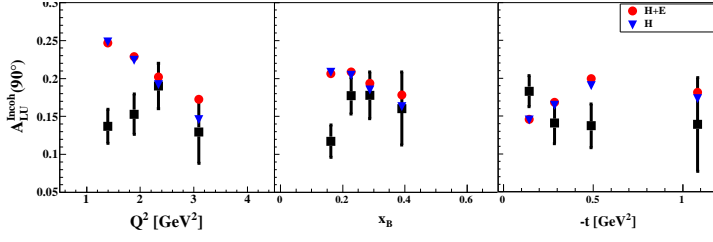


**Fig. 7** Azimuthal beam-spin asymmetry for the proton in  ${}^4\text{He}$ ,  $A_{LU}^{Incoh}$ , eq. 14, for  $\phi = 90^\circ$ : results presented in ref. [53] (red dots), results updated including also the contribution of the GPD  $E$  (blue triangles), compared with data (black squares) [15]. Data and our results are represented in the experimental bins, from left to right, for  $Q^2$ ,  $x_B = Q^2/(2M\nu)$  and  $t = \Delta^2$ .

BSA reads

$$A_{LU}^{Incoh} = \frac{\int_{exp} dE d\mathbf{p} P^{4He}(\mathbf{p}, E) g(\mathbf{p}, E, K) \mathcal{I}_{DVCS-BH}}{\int_{exp} dE d\mathbf{p} P^{4He}(\mathbf{p}, E) g(\mathbf{p}, E, K) T_{BH}^2} \equiv \frac{\mathcal{I}_{DVCS-BH}^{4He}}{T_{BH}^{2^{4He}}} \quad (14)$$

For an exhaustive comparison with the experimental data, the azimuthal dependence of eq. 14, given by the decomposition in  $\phi$  harmonics of the interference and the BH part, has been exploited. Information about the parton content of the bound proton enters only the interference term, i.e.  $\mathcal{I}_{DVCS-BH} \propto \Im m \mathbf{H}_q(\xi', t)$ . This term accounts for the modification to the partonic structure through the skewness  $\xi' = \frac{-q^2}{P \cdot q}$ , where the off-shellness and the dependence on the 3-momentum components of the bound proton, affected by nuclear effects, enter. In the CFF  $\mathbf{H}_q(\xi, t)$ , contributions from the GPDs  $H$  and  $E$ , for which we made use of the GK models [50, 56], has been included in the present results. As for the coherent channel, the contribution from the GPD  $E$ , not already included in refs. [53, 54], turns out to be very small at the considered kinematics. The results are depicted in Fig. 7. As expected, the agreement with experimental data is good except the region of lowest  $Q^2$  where the impulse approximation exposes its limitations and FSI effects could be considerable. In order to estimate how nuclear effects affect the obtained results, i.e. if they are related to some medium modification of the inner parton structure described by the GPD, we considered the ratio between the BSA for a bound nucleon, given by eq. 14 and that for a free proton (labelled with the superscript  $p$ ):

$$\frac{A_{LU}^{Incoh}}{A_{LU}^p} \propto \frac{\mathcal{I}_{DVCS-BH}^{4He}}{\mathcal{I}_{DVCS-BH}^p} \frac{T_{BH}^{2^p}}{T_{BH}^{2^{4He}}} = \frac{(nucl.eff.)_{Int}}{(nucl.eff.)_{BH}}. \quad (15)$$

As a matter of facts, the above *super ratio* is proportional to the ratio of the nuclear effects on the BH and DVCS interference to the nuclear effects on the BH cross section. If the nuclear dynamics modifies the  $\mathcal{I}_{DVCS-BH}^{4He}$  and  $T_{BH}^{2^{4He}}$

cross sections in a different way, the effect can be big even if the parton structure of the bound proton does not change appreciably. However, such effects could be dramatically reduced and hidden in the *super ratio*.

This is what we definitely obtained: within our IA approach, both in the BH and in the interference amplitudes big nuclear effects occur that are cancelled out in the *super ratio*. Such effects seem to be related to kinematical nuclear effects, foreseen in a conventional nuclear physics scenario, rather than to medium modifications of the parton structure due exotic effects, such as dynamical off-shellness. More detailed studies in this sense are presented in ref. [54] where also checks for the stability of our model, using different ingredients both for the nuclear part and the nucleonic GPDs models, have been performed. Concerning this latter ingredient as well as the relevant GPD  $E_q^N$ , use has been made of the virtual access infrastructure 3DPARTONS [63].

## 4 Perspectives

Since the time of the first measurements of nuclear GPDs, performed by the HERMES collaboration in DESY [36], which could not differentiate coherent and incoherent channels directly and had to rely on the dominance of either channel at small and large  $t$ , a crucial step forward has been performed by the data released by the CLAS collaboration at JLab, successful in distinguishing coherent and incoherent DVCS channels exclusively [64, 14, 15]. The analysis clearly shows only a small coverage in  $x_{Bj}$  and  $t$  and we should expect that an extension of this program with the upgraded CLAS12 will provide a large data set to analyze the GPDs of light nuclei in the valence region, with much smaller errorbars, given the luminosity gain. Farther in the future, the EIC in the US [4] will be the perfect facility to study nuclear DVCS. Indeed, thanks to the collider kinematics, it will be much easier to detect the recoiling nuclei and to polarize the incoming nuclear beams. In addition, the high energy available at the EIC will allow to cleanly map the nuclear GPDs at low  $x$ , including also the gluon GPDs. Besides, as for any coherent exclusive process, in DVCS off nuclei the collider setup will make easy the detection of the recoiling intact nucleus, which is very slow in a fixed target experiment. This is even more important in the incoherent channel, for which the detection of other nuclear fragments could allow to control FSI effects.

The study of nuclear GPDs is a fascinating subject, already deeply studied theoretically, as described in this paper. At the same time, its actual experimental investigation has just started and, in the near future, exciting updates to the material presented here are expected. With the operation of light nuclear beams at the EIC, the involvement of the Few-Body Physics community will become more and more important.

**Acknowledgements** We gratefully acknowledge the collaboration with R. Dupré and M. Viviani, and many crucial discussions with E. Voutier and M. Hattawy on the Jefferson Lab experiments. S.F. thanks P. Sznajder and C. Mezrag for some tuition on the use of

the virtual access infrastructure 3DPARTONS, funded by the European Union’s Horizon 2020 research and innovation programme under grant agreement No 824093. This work was supported in part by the STRONG-2020 project of the European Union’s Horizon 2020 research and innovation programme under grant agreement No 824093, Working Package 23, ”GPDS-ACT” and by the project ”Deeply Virtual Compton Scattering off  $^4\text{He}$ ”, in the programme FRB of the University of Perugia.

## References

- [1] I.C. Cloët et al. “Exposing Novel Quark and Gluon Effects in Nuclei”. In: *J. Phys. G* 46.9 (2019), p. 093001. DOI: 10.1088/1361-6471/ab2731. arXiv: 1902.10572 [nucl-ex].
- [2] J. J. Aubert et al. “The ratio of the nucleon structure functions  $F_{2,n}$  for iron and deuterium”. In: *Phys. Lett.* B123 (1983), p. 275. DOI: 10.1016/0370-2693(83)90437-9.
- [3] R. Dupré and S. Scopetta. “3D Structure and Nuclear Targets”. In: *Eur. Phys. J. A* 52.6 (2016), p. 159. DOI: 10.1140/epja/i2016-16159-1. arXiv: 1510.00794 [nucl-ex].
- [4] A. Accardi et al. “Electron Ion Collider: The Next QCD Frontier: Understanding the glue that binds us all”. In: *Eur. Phys. J. A* 52.9 (2016). Ed. by A. Deshpande, Z.E. Meziani, and J.W. Qiu, p. 268. DOI: 10.1140/epja/i2016-16268-9. arXiv: 1212.1701 [nucl-ex].
- [5] Dieter Müller et al. “Wave functions, evolution equations and evolution kernels from light ray operators of QCD”. In: *Fortsch. Phys.* 42 (1994), pp. 101–141. DOI: 10.1002/prop.2190420202. arXiv: hep-ph/9812448.
- [6] Xiang-Dong Ji. “Gauge-Invariant Decomposition of Nucleon Spin”. In: *Phys. Rev. Lett.* 78 (1997), pp. 610–613. DOI: 10.1103/PhysRevLett.78.610. arXiv: hep-ph/9603249.
- [7] A.V. Radyushkin. “Scaling limit of deeply virtual Compton scattering”. In: *Phys. Lett. B* 380 (1996), pp. 417–425. DOI: 10.1016/0370-2693(96)00528-X. arXiv: hep-ph/9604317.
- [8] K. Goeke, Maxim V. Polyakov, and M. Vanderhaeghen. “Hard exclusive reactions and the structure of hadrons”. In: *Prog.Part.Nucl.Phys.* 47 (2001), pp. 401–515. DOI: 10.1016/S0146-6410(01)00158-2. arXiv: hep-ph/0106012 [hep-ph].
- [9] M. Diehl. “Generalized parton distributions in impact parameter space”. In: *Eur. Phys. J.* C25 (2002). [Erratum: *Eur. Phys. J.* C31,277(2003)], pp. 223–232. DOI: 10.1007/s10052-002-1016-9. arXiv: hep-ph/0205208 [hep-ph].
- [10] A.V. Belitsky and A.V. Radyushkin. “Unraveling hadron structure with generalized parton distributions”. In: *Phys. Rept.* 418 (2005), pp. 1–387. DOI: 10.1016/j.physrep.2005.06.002. arXiv: hep-ph/0504030.
- [11] Sigfrido Boffi and Barbara Pasquini. “Generalized parton distributions and the structure of the nucleon”. In: *Riv. Nuovo Cim.* 30 (2007), p. 387. DOI: 10.1393/ncr/i2007-10025-7. arXiv: 0711.2625 [hep-ph].
- [12] Matthias Burkardt. “Impact parameter dependent parton distributions and off forward parton distributions for zeta  $\rightarrow 0$ ”. In: *Phys. Rev.* D62 (2000). [Erratum: *Phys. Rev.* D66,119903(2002)], p. 071503. DOI:

- 10.1103/PhysRevD.62.071503, 10.1103/PhysRevD.66.119903. arXiv: hep-ph/0005108 [hep-ph].
- [13] Raphaël Dupré et al. “Analysis of Deeply Virtual Compton Scattering Data at Jefferson Lab and Proton Tomography”. In: *Eur. Phys. J. A* 53.8 (2017), p. 171. DOI: 10.1140/epja/i2017-12356-8. arXiv: 1704.07330 [hep-ph].
- [14] M. Hattawy et al. “First Exclusive Measurement of Deeply Virtual Compton Scattering off  $^4\text{He}$ : Toward the 3D Tomography of Nuclei”. In: *Phys. Rev. Lett.* 119.20 (2017), p. 202004. DOI: 10.1103/PhysRevLett.119.202004. arXiv: 1707.03361 [nucl-ex].
- [15] M. Hattawy et al. “Exploring the Structure of the Bound Proton with Deeply Virtual Compton Scattering”. In: *Phys. Rev. Lett.* 123.3 (2019), p. 032502. DOI: 10.1103/PhysRevLett.123.032502. arXiv: 1812.07628 [nucl-ex].
- [16] Edgar R. Berger et al. “Generalized parton distributions in the deuteron”. In: *Phys. Rev. Lett.* 87 (2001), p. 142302. DOI: 10.1103/PhysRevLett.87.142302. arXiv: hep-ph/0106192 [hep-ph].
- [17] M.V. Polyakov. “Generalized parton distributions and strong forces inside nucleons and nuclei”. In: *Phys. Lett.* B555 (2003), pp. 57–62. DOI: 10.1016/S0370-2693(03)00036-4. arXiv: hep-ph/0210165 [hep-ph].
- [18] Ju-Hyun Jung et al. “In-medium modified energy-momentum tensor form factors of the nucleon within the framework of a  $\pi$ - $\rho$ - $\omega$  soliton model”. In: *Phys. Rev.* D89.11 (2014), p. 114021. DOI: 10.1103/PhysRevD.89.114021. arXiv: 1402.0161 [hep-ph].
- [19] Maxim V. Polyakov and Peter Schweitzer. “Forces inside hadrons: pressure, surface tension, mechanical radius, and all that”. In: *Int. J. Mod. Phys. A* 33.26 (2018), p. 1830025. DOI: 10.1142/S0217751X18300259. arXiv: 1805.06596 [hep-ph].
- [20] A. Accardi et al. “ $e^+$ @JLab White Paper: An Experimental Program with Positron Beams at Jefferson Lab”. In: (July 2020). arXiv: 2007.15081 [nucl-ex].
- [21] Whitney Armstrong et al. “Partonic Structure of Light Nuclei”. In: (Aug. 2017). arXiv: 1708.00888 [nucl-ex].
- [22] M. Rinaldi and S. Scopetta. “Extracting generalized neutron parton distributions from  $^3\text{He}$  data”. In: *Phys. Rev.* C87.3 (2013), p. 035208. DOI: 10.1103/PhysRevC.87.035208. arXiv: 1208.2831 [nucl-th].
- [23] K. Goeke, V. Guzey, and M. Siddikov. “Leading twist nuclear shadowing, nuclear generalized parton distributions and nuclear DVCS at small  $x$ ”. In: *Phys. Rev.* C79 (2009), p. 035210. DOI: 10.1103/PhysRevC.79.035210. arXiv: 0901.4711 [hep-ph].
- [24] F. Cano and B. Pire. “Deep electroproduction of photons and mesons on the deuteron”. In: *Eur. Phys. J.* A19 (2004), pp. 423–438. DOI: 10.1140/epja/i2003-10127-x. arXiv: hep-ph/0307231 [hep-ph].
- [25] V. Guzey and M. Strikman. “DVCS on spinless nuclear targets in impulse approximation”. In: *Phys. Rev.* C68 (2003), p. 015204. DOI: 10.1103/PhysRevC.68.015204. arXiv: hep-ph/0301216 [hep-ph].

- [26] A. Kirchner and Dieter Mueller. “Deeply virtual Compton scattering off nuclei”. In: *Eur. Phys. J. C* 32 (2003), pp. 347–375. DOI: 10.1140/epjc/s2003-01415-x. arXiv: hep-ph/0302007.
- [27] Sergio Scopetta. “Generalized parton distributions of He-3”. In: *Phys.Rev. C* 70 (2004), p. 015205. DOI: 10.1103/PhysRevC.70.015205. arXiv: nucl-th/0404014 [nucl-th].
- [28] S. Liuti and S.K. Taneja. “Microscopic description of deeply virtual Compton scattering off spin-0 nuclei”. In: *Phys.Rev. C* 72 (2005), p. 032201. DOI: 10.1103/PhysRevC.72.032201. arXiv: hep-ph/0505123 [hep-ph].
- [29] Sara Fucini, Sergio Scopetta, and Michele Viviani. “Coherent deeply virtual Compton scattering off  $^4\text{He}$ ”. In: *Phys. Rev. C* 98.1 (2018), p. 015203. DOI: 10.1103/PhysRevC.98.015203. arXiv: 1805.05877 [nucl-th].
- [30] K. S. Egiyan et al. “Measurement of 2- and 3-nucleon short range correlation probabilities in nuclei”. In: *Phys. Rev. Lett.* 96 (2006), p. 082501. DOI: 10.1103/PhysRevLett.96.082501. arXiv: nucl-ex/0508026 [nucl-ex].
- [31] R. Subedi et al. “Probing Cold Dense Nuclear Matter”. In: *Science* 320 (2008), pp. 1476–1478. DOI: 10.1126/science.1156675. arXiv: 0908.1514 [nucl-ex].
- [32] O. Hen et al. “Measurement of transparency ratios for protons from short-range correlated pairs”. In: *Phys. Lett.* B722 (2013), pp. 63–68. DOI: 10.1016/j.physletb.2013.04.011. arXiv: 1212.5343 [nucl-ex].
- [33] Stanley J. Brodsky, Francis E. Close, and J.F. Gunion. “Phenomenology of Photon Processes, Vector Dominance and Crucial Tests for Parton Models”. In: *Phys.Rev. D* 6 (1972), p. 177. DOI: 10.1103/PhysRevD.6.177.
- [34] M.V. Polyakov and A.G. Shuvaev. “On’dual’ parametrizations of generalized parton distributions”. In: (2002). arXiv: hep-ph/0207153 [hep-ph].
- [35] V. Guzey and M. Siddikov. “On the A-dependence of nuclear generalized parton distributions”. In: *J.Phys.* G32 (2006), pp. 251–268. DOI: 10.1088/0954-3899/32/3/002. arXiv: hep-ph/0509158 [hep-ph].
- [36] A. Airapetian et al. “Nuclear-mass dependence of azimuthal beam-helicity and beam-charge asymmetries in deeply virtual Compton scattering”. In: *Phys.Rev. C* 81 (2010), p. 035202. DOI: 10.1103/PhysRevC.81.035202. arXiv: 0911.0091 [hep-ex].
- [37] V. Guzey. “Neutron contribution to nuclear DVCS asymmetries”. In: *Phys. Rev. C* 78 (2008), p. 025211. DOI: 10.1103/PhysRevC.78.025211. arXiv: 0801.3235 [nucl-th].
- [38] S. Niccolai et al. “Deeply Virtual Compton Scattering on the Neutron with CLAS12 at 11 GeV”. In: *Proposal 12-11-003 at JLab PAC 37* (2011).
- [39] K. Hafidi et al. “Nuclear Exclusive and Semi-inclusive Physics with a New CLAS12 Low Energy Recoil Detector”. In: *Letter of Intent 12-10-009 to the JLab PAC 35* (2009).
- [40] S. Kuhn et al. “The structure of the free neutron via spectator tagging”. In: *E12-06-113, JLAB approved experiment* (2006).
- [41] Swadhin K. Taneja et al. “Angular momentum sum rule for spin one hadronic systems”. In: *Phys. Rev. D* 86 (2012), p. 036008. DOI: 10.1103/PhysRevD.86.036008. arXiv: 1101.0581 [hep-ph].

- [42] W. Cosyn and B. Pire. “Transversity generalized parton distributions for the deuteron”. In: *Phys. Rev. D* 98.7 (2018), p. 074020. DOI: 10.1103/PhysRevD.98.074020. arXiv: 1806.01177 [hep-ph].
- [43] W. Cosyn, A. Freese, and B. Pire. “Polynomiality sum rules for generalized parton distributions of spin-1 targets”. In: *Phys. Rev. D* 99.9 (2019), p. 094035. DOI: 10.1103/PhysRevD.99.094035. arXiv: 1812.01511 [hep-ph].
- [44] Wim Cosyn et al. “The energy-momentum tensor of spin-1 hadrons: formalism”. In: *Eur. Phys. J. C* 79.6 (2019), p. 476. DOI: 10.1140/epjc/s10052-019-6981-3. arXiv: 1903.00408 [hep-ph].
- [45] S. Scopetta. “Conventional nuclear effects on generalized parton distributions of trinucleons”. In: *Phys. Rev. C* 79 (2009), p. 025207. DOI: 10.1103/PhysRevC.79.025207. arXiv: 0901.3058 [nucl-th].
- [46] M. Rinaldi and S. Scopetta. “Neutron orbital structure from generalized parton distributions of  $^3\text{He}$ ”. In: *Phys. Rev. C* 85 (2012), p. 062201. DOI: 10.1103/PhysRevC.85.062201. arXiv: 1204.0723 [nucl-th].
- [47] Matteo Rinaldi and Sergio Scopetta. “Theoretical description of deeply virtual Compton scattering off  $^3\text{He}$ ”. In: *Few Body Syst.* 55 (2014), pp. 861–864. DOI: 10.1007/s00601-014-0803-9. arXiv: 1401.1350 [nucl-th].
- [48] Alessio Del Dotto et al. “Light-Front spin-dependent Spectral Function and Nucleon Momentum Distributions for a Three-Body System”. In: *Phys. Rev. C* 95.1 (2017), p. 014001. DOI: 10.1103/PhysRevC.95.014001. arXiv: 1609.03804 [nucl-th].
- [49] Robert B. Wiringa, V. G. J. Stoks, and R. Schiavilla. “An Accurate nucleon-nucleon potential with charge independence breaking”. In: *Phys. Rev. C* 51 (1995), pp. 38–51. DOI: 10.1103/PhysRevC.51.38. arXiv: nucl-th/9408016 [nucl-th].
- [50] S. V. Goloskokov and P. Kroll. “The Role of the quark and gluon GPDs in hard vector-meson electroproduction”. In: *Eur. Phys. J. C* 53 (2008), pp. 367–384. DOI: 10.1140/epjc/s10052-007-0466-5. arXiv: 0708.3569 [hep-ph].
- [51] S. Liuti and S. K. Taneja. “Generalized parton distributions and color transparency phenomena”. In: *Phys. Rev. D* 70 (2004), p. 074019. DOI: 10.1103/PhysRevD.70.074019. arXiv: hep-ph/0405014 [hep-ph].
- [52] B.S. Pudliner et al. “Quantum Monte Carlo calculations of  $A \leq 6$  nuclei”. In: *Phys. Rev. Lett.* 74 (1995), pp. 4396–4399. DOI: 10.1103/PhysRevLett.74.4396. arXiv: nucl-th/9502031.
- [53] Sara Fucini, Sergio Scopetta, and Michele Viviani. “Catching a glimpse of the parton structure of the bound proton”. In: *Phys. Rev. D* 101.7 (2020), p. 071501. DOI: 10.1103/PhysRevD.101.071501. arXiv: 1909.12261 [nucl-th].
- [54] Sara Fucini, Sergio Scopetta, and Michele Viviani. “Incoherent deeply virtual Compton scattering off  $^4\text{He}$ ”. In: (Aug. 2020). arXiv: 2008.11437 [nucl-th].
- [55] Wiki page for the Yellow Report Physics Working group. 2020. URL: [https://wiki.bnl.gov/eicug/index.php/Yellow\\_Report\\_Physics\\_Exclusive\\_Reactions](https://wiki.bnl.gov/eicug/index.php/Yellow_Report_Physics_Exclusive_Reactions).
- [56] S.V. Goloskokov and P. Kroll. “The Target asymmetry in hard vector-meson electroproduction and parton angular momenta”. In: *Eur. Phys. J. C* 59 (2009), pp. 809–819. DOI: 10.1140/epjc/s10052-008-0833-x. arXiv: 0809.4126 [hep-ph].

- 
- [57] Hiko Morita and Toru Suzuki. “A realistic spectral function of He-4”. In: *Prog. Theor. Phys.* 86 (1991), pp. 671–684. DOI: 10.1143/PTP.86.671.
- [58] Victor D. Efros, Winfried Leidemann, and Giuseppina Orlandini. “Exact He-4 spectral function in a semirealistic N N potential model”. In: *Phys. Rev. C* 58 (1998), pp. 582–585. DOI: 10.1103/PhysRevC.58.582. arXiv: nucl-th/9805002.
- [59] M. Viviani, A. Kievsky, and A. Rinat. “GRS computation of deep inelastic electron scattering on He-4”. In: *Phys. Rev. C* 67 (2003), p. 034003. DOI: 10.1103/PhysRevC.67.034003. arXiv: nucl-th/0111049.
- [60] A. Kievsky, S. Rosati, and M. Viviani. “The three nucleon bound state with realistic soft core and hard core potentials”. In: *Nucl. Phys. A* 551 (1993), pp. 241–254. DOI: 10.1016/0375-9474(93)90480-L.
- [61] M. Viviani, A. Kievsky, and S. Rosati. “Calculation of the alpha-particle ground state within the hyperspherical harmonic basis”. In: *Phys. Rev. C* 71 (2005), p. 024006. DOI: 10.1103/PhysRevC.71.024006. arXiv: nucl-th/0408019.
- [62] A. Kievsky et al. “A High-precision variational approach to three- and four-nucleon bound and zero-energy scattering states”. In: *J. Phys. G* 35 (2008), p. 063101. DOI: 10.1088/0954-3899/35/6/063101. arXiv: 0805.4688 [nucl-th].
- [63] B. Berthou et al. “PARTONS: PARTonic Tomography Of Nucleon Software: A computing framework for the phenomenology of Generalized Parton Distributions”. In: *Eur. Phys. J. C* 78.6 (2018), p. 478. DOI: 10.1140/epjc/s10052-018-5948-0. arXiv: 1512.06174 [hep-ph].
- [64] Eric Voutier. “Helium Compton Form Factor Measurements at CLAS”. In: *PoS DIS2013* (2013), p. 057. arXiv: 1307.0222 [nucl-ex].

